Full Paper

Version: May 3, 2018

Data-driven mathematical modeling of the effect of particle size distribution on the transitory reaction kinetics of hot metal desulfurization

Tero Vuolio [1)]*, Ville-Valtteri Visuri [1)], Sakari Tuomikoski [2)], Timo Paananen [2)] and Timo Fabritius [1)]

Abstract

The aim of this work was to develop a prediction model for hot metal desulfurization. More specifically, the study aimed at finding a set of explanatory variables that are mandatory in prediction of the kinetics of the lime-based transitory desulfurization reaction and evolution of the sulfur content in the hot metal. The prediction models were built through multivariable analysis of process data and phenomena-based simulations. The model parameters for the suggested model types are identified by solving multivariable least-squares cost-functions with suitable solution strategies. One conclusion we arrived at was that in order to accurately predict the rate of desulfurization, it is necessary to know the particle size distribution of the desulfurization reagent. It was also observed that a genetic algorithm can be successfully applied in numerical parameter identification of the proposed model type. It was found that even a very simplistic parameterized expression for the 1st order rate constant provides more accurate prediction for the end content of sulfur compared to more complex models, if the data-set applied for the modeling contains the adequate information.

Keywords: hot metal desulfurization, dynamic modeling, multivariable analysis, model parameter identification, numerical solution strategies, rate phenomena, lime-based reagents

1) Process Metallurgy Research Unit, University of Oulu, P.O. Box 4300, FI–90014, University of Oulu, Finland.

2) SSAB Europe Oy, Rautaruukintie 155, P.O. Box 93, FI–92101, Raahe, Finland.

*) Corresponding author. E-mail: tero.vuolio@oulu.fi

I. INTRODUCTION

In blast furnace-based steel production, sulfur is considered one of the main impurities in hot metal. In powder injection, a desulfurization reagent is injected into hot metal with the help of an inert carrier gas through an immersed lance. Suitable desulfurization reagents include lime, calcium carbide, magnesium, soda ash, limestone and zinc oxide. [4] The focus of this study is on lime- and limestone-based desulfurization reagents.

The effect of particle size distribution on the rate of desulfurization reaction has not been extensively studied in the case of lime-based desulfurization reagents. In the studies conducted by Coudure and Irons [3], Lindström and Sichen [4] and Shevchenko *et al.* [2], it was postulated that decreasing the particle size of a desulfurization reagent increases the extraction capacity of the material. The studies conducted by Lindström and Sichen [18] indicate that a smaller particle size provides improved reaction kinetics between solid lime and sulfur, although the study considers only the solid-state diffusion controlled phase, which is not considered the only rate-controlling mechanism in the injection-based industrial hot metal desulfurization. In addition, the authors were not able to extract the effect of a fluidizing element on the efficiency of a fine-grade lime-based reagent, and so could not give a quantitative description of the variables that determine the overall reaction kinetics in the full-scale process. Most importantly, the experiments were conducted with constant process parameters and in a two-phase system (reagent-metal), whereas the industrial hot metal desulfurization carried out with powder injection can be considered a three-phase system (metal-gas-reagent), in which the carrier-gas potentially affects the desulfurization reaction by preventing a direct metal-reagent contact. [3-4]

The studies conducted by Coudure and Irons [3] concerned only the kinetics of calcium carbide, and so their results are only partially comparable to the results of this study. Shevchenko *et al.*[2] found out that material efficiency of a more fine-grade lime with a diameter less than 100 µm is higher than the corresponding efficiency of more coarse particles, but the authors did not consider the extent to which the finer gradation of lime might improve the desulfurization kinetics. In addition, the methodology applied for determining the particle size distribution of lime was a sieving-analysis with only a few sieve classes, which gives a relatively inaccurate approximation of the full particle size distribution of the material. [4]

Vinoo *et al.*[22] applied multivariable regression modeling for predicting the evolution of the sulfur content of the metal bath in the case of a calcium carbide reagent. However, the authors did not apply the properties of the injected reagent as a predictor variable, which assumedly decreases the accuracy of the model especially in continuous production, as the reagent properties cannot be assumed constant. The authors found that the variables affecting the efficiency of desulfurization could be described in terms of simple linear interactions in pre-classified operational temperatures, as a result of which the rate of desulfurization predicted by the model does obey the mass-transfer laws only in certain linearized operational states. In addition, the prediction error of the model was relatively large (± 0.003% units), and was based on the validation data of 15 treatments only. [22]

Rastogi *et al.* [28], Deo *et al.* [29] and Datta *et al.* [15] applied genetic algorithms and artificial neural networks in the identification of hot metal desulfurization prediction models. The authors managed to identify the most significant reaction mechanisms based on the industrial data [28], and several other assumedly significant explanatory variables, but excluded the particle size distribution of the reagent from the data set. [29, 15] As the significance of particle size distribution as a suitable explanatory variable candidate has been confirmed in several studies [2, 3, 4, 17, 18], the absence of it assumedly resulted in a relative poor predictive power of the approach, regardless of the complex model structure. [22, 28, 29, 15]

In this paper, the hot metal desulfurization is analyzed concurrently with data-driven and phenomena-based modeling. In mathematical modeling of hot metal desulfurization, there are certain obscurities related to phenomena occurring in the hot metal ladle. For this reason, fully phenomena-based models with evaluative fitting parameters, and without accurate determination of the particle size distribution, often fail to predict the end content of sulfur precisely.[6, 9, 22, 28-29] Moreover, mathematical models that are based on exhaustive descriptions of the physical and chemical fundamentals – especially those that provide a detailed solution of the fluid flow field – tend to be computationally heavy and unsuited to day-to-day process control.

The objective of this study is to develop a mathematical description with a high prediction performance based on a comprehensive analysis of system kinetics. The scope of the study is limited to the proper form of the prediction model, and to the set of explanatory variables that

are relevant for the prediction of the final sulfur content and kinetics of desulfurization. In particular, the model aims to account for the effect of the reagent particle size distribution and certain operating variables on the kinetics of the transitory reaction.

The parameters for the suggested model types are identified by minimizing a multivariable least-squares cost-function using the suitable solution strategies. The process data for analysis, fitting and validation of the models is gathered from the primary desulfurization process at SSAB Raahe, Finland. All the algorithms and suggested solution strategies have been programmed with Matlab®.

II. METHODOLOGY

Given a large data set with high number of variables, finding the suitable set of features that describe accurately enough the changes in the output variable is a complex task. With high-dimensional data sets there is often a risk of selecting irrelevant, noisy or collinear variables, which often results in a poorly interpretable model or weakened model performance. There are standardized methods for determining a proper set of variable which can be further categorized as manual and automatized feature selection methods. [8] In this work, the analysis and variable selection procedure is carried out in such a way that the variables chosen in the parameterized prediction models are partially extracted with manual feature selection, by applying the results of the simulations based on a theoretical description of the transitory reaction kinetics.

A. *System identification based on the rate of transitory reaction*

Hot metal desulfurization with powder injection consists of two main reactions: [11]

i) Transitory contact reaction (reagent-metal)

ii) Permanent contact reaction (slag-metal)

The kinetics of the desulfurization reaction is determined as a sum of reaction rates k_i and k_{ii}, but due to the fact that in the case of powder injection the large interfacial area, determined by numerous spherical particles, for mass transfer results that $k_i >> k_{ii}$, which is why the permanent contact reaction can often be neglected from the overall kinetics. [6, 11, 26, 28] In some studies, the reaction between the particles entrapped in the carrier-gas bubbles and the hot metal is also considered as one of the main mechanisms, but the contribution of the entrapped

particles on the overall kinetics has been studied to be negligible. [3, 21, 28] In the case of a transitory desulfurization reaction with a solid lime-based reagent, the calcium oxide is converted into sulfide by a following ion-exchange reaction: [1]

$$< CaO > + [S] \rightarrow < CaS > + [O] \quad [1]$$

The transitory reaction is often considered to follow first order reaction kinetics, by assuming the mass transfer related control of the reaction rate. Based on the previous research, the rate constant for hot metal desulfurization carried out with powder injection can be summarized to be mainly a function of the following parameters: [1-7, 9, 12-15, 17]

- active solid surface area in contact with the metal phase,
- feed rate of the particles,
- mass of the metal bath,
- total flow rate of the gaseous compounds,
- mass transfer coefficient in the metal-reagent diffusion boundary layer,
- rate of solid-state diffusion in the product phase, and
- average residence time of the reagent particles in the metal bath.

Various studies [3, 5, 6, 9, 26] have found the transitory desulfurization reaction to be controlled by mass transfer in the hot metal boundary layer. However, as the reaction proceeds, the diffusion of sulfur and calcium ions inside the CaS layer determines the rate of reaction as the slowest step of mass transfer. [1, 6] Delhey et al.[52] studied hot metal desulphurization with lime and calcium carbide according to the lance injection process. In general, the desulphurization efficiency increased non-linearly as a function of the amount of reagent injected. [52] For a given injection rate, the efficiency of desulphurization increased with a higher lance depth. [52] The increase in rate constant was not found to be linearly dependent on the estimated residence time of the particles, and consequently it was suggested that the deposition of the reaction product on the surface of the reagent hindered the increase in reaction rate. [52] As for lime, the desulphurization efficiency was found to be increased with a higher Al content of the metal bath. [52]

Although, with very high injection rates a fresh solid surface is continuously introduced in the melt, which assumedly increases the rate of desulfurization during the solid-state diffusion control. For this reason, the boundary-layer diffusion assumption is applicable in several situations, especially when applying relatively large particles in the injection and high injection rates of the solid reagent. As the desulfurization is assumed to follow first order reaction kinetics, the dynamic changes in the sulfur concentration of hot metal phase can be written as a lumped parameter model, where the sulfur concentration in the melt approaches the equilibrium concentration of sulfur:

$$\frac{\mathrm{d}[\mathrm{S}]}{\mathrm{d}t} = -k_{\mathrm{tot}}([\mathrm{S}] - [\mathrm{S}]_{\mathrm{eq}}), \qquad [2]$$

where $\boldsymbol{k_{\mathrm{tot}}}$ is the rate constant for transitory desulfurization reaction, [S] is the sulfur concentration and $[\mathrm{S}]_{\mathrm{eq}}$ is the equilibrium sulfur concentration. The **Eq. 2** can be re-arranged and integrated over the concentration gradient and treatment time. The analytical solution for the dynamic sulfur concentration is therefore

$$[\mathrm{S}]_t = \left([\mathrm{S}]_0 - [\mathrm{S}]_{\mathrm{eq}}\right) \exp(-k_{\mathrm{tot}} t) + [\mathrm{S}]_{\mathrm{eq}}, \qquad [3]$$

where $[\mathrm{S}]_0$ is the initial sulfur concentration in the melt. Moreover, the rate constant for the transitory reaction can be formulated as:

$$k_{\mathrm{tot}} = -\frac{1}{t} \ln\left(\frac{[\mathrm{S}]_t - [\mathrm{S}]_{\mathrm{eq}}}{[\mathrm{S}]_0 - [\mathrm{S}]_{\mathrm{eq}}}\right), \qquad [4]$$

B. *Particle size class specific rate constant*

In a fully theoretic approach, the values of predicted particle size class specific rate constants are more or less trivial, as the residence-times and the number of injected particles that get into contact with the melt are complex to determine accurately without extensive experiments or computational fluid dynamics simulations. For this reason, the mathematical models often apply evaluative fitting parameters in the prediction. [6, 9] The problem of this approach in dynamic process control is that the proposed fitting parameters are a function of operational

variables, such as flow rate of the injection gas, mass flow rate of the reagent and amount of co-injected gas-releasing agents, all of which affect to the convective flows in the system. Based on a simplified surface-area approach, the rate constant for a single particle size class can be written as: [6]

$$k_{i,d_p} = \beta_{[S]} \frac{6}{d_p} \frac{\dot{m}_r}{m_{Fe}} \frac{\rho_{Fe}}{\rho_r} t_{res}, \quad [5]$$

where k_{i,d_p} is the particle size class specific rate constant, $\dot{m}_r$ is the particle class specific feed-rate, m_{Fe} is the mass of the hot metal, t_{res} is the average residence time of the particle in the melt and ρ_j is the density of a phase j. It should be noted that the term $6/d_p$ corresponds to $(A/V)_p$ in the case of a sphere. In this formulation, the residence time of the single particle size class acts as an unknown fitting parameter. In the surface-area approach, the rate constant is assumed inversely proportional to diameter of a reagent particle, and thus $k_{i,d_p} \rightarrow \infty$ as $d_p \rightarrow 0$. **Eq. 5** gives the rate constant for a single size class, which is prediction models of this kind often apply a suitable mean size class for the mean diameter. [3, 6, 9] The surface-based mean diameter ($d_{32} = 6/d_p$) is also known as the Sauter mean diameter (SMD).

In the case of an example particle size distribution applied in this study, the calculated values for Sauter mean diameter are even as small as $d_{32} \approx 4$ μm. So as the rate of mass transfer is mostly determined by the surface area between the emulsified discrete phase and the continuous phase, the Sauter mean diameter often drastically overestimates the rate constant. This is because the solid surface area of the injected material is often significantly larger than the surface area that actually takes part in the reactions. In several cases, the theoretical single particle models applying the Sauter mean diameter in a prediction of the rate constant for the transitory reaction the values are overestimated.

The expression for the rate constant also suggests that all of the reagent particles get into contact with the melt, and thus the rate constant of a particle size class is directly proportional to the solid injection rate. The formulation also treats assumedly an emulsified system as a non-emulsified, and so the rate constant is valid only when the thermodynamic extraction capacity for a single size class is very small, which corresponds to a situation where the desulfurization reaction is truly controlled by boundary-layer diffusion instead of solid-state diffusion. With short average residence-times, this approach can be considered valid, as the formed CaS layers around the particle are relatively thin. [1, 6] To treat the time constant in the

case of a full particle size distribution, the volume based rate constant can be written as a weighted sum of particle size class specific time constants:

$$k_{\mathrm{tot}} = \sum_{i=0}^{n} \Phi_i y_i k_{i,d_p}, \qquad [6]$$

where Φ_i is a binary variable determined from the contact criteria for a particle size class i, y_i is the volume fraction of particle class i. The rate constant for a particle size class i is yield by weighting the solids flow rate with the mass-fraction of a size class i in the cumulative distribution as follows:

$$\Phi y_i k_{i,d_p} = \Phi \beta_{[\mathrm{S}]} \frac{6}{d_p} \frac{\dot{m}_r}{m_{\mathrm{Fe}}} \frac{\rho_{\mathrm{Fe}}}{\rho_r} t_{\mathrm{res}} (R_{i+1} - R_i). \qquad [7]$$

The rate constant for the injected particles following a certain particle size distribution can be predicted by applying a mathematical description to the cumulative particle size distribution. In this study, the particle size distribution was described with Rosin-Rammler-Sperling-distribution (RRS). The cumulative mass fraction of a particle size class i in the size distribution can be expressed by applying d_{80} as the fineness parameter as follows:

$$R_i = 0.2^{\left[\left(\frac{d_{80}}{d_p}\right)^n\right]}, \qquad [8]$$

where R_i is the cumulative mass fraction of a particle size class i, d_{80} is the particle size corresponding to percentage below 80% in the overall distribution and n is the spreading-parameter that describes the homogeneity of the distribution. The fineness-parameter can be solved as a general least-squares optimization problem based on the characteristic particle size distribution.

C. *Mass-transfer around the dispersed phase*

As the surface-based mean can often give highly overestimated results, the particle size distribution can be averaged by taking account the mass-transfer inside the boundary-layer. Coudure and Irons [3] proposed a particle mean diameter based on the Sherwood-number and the expression of the rate constant for the transitory reaction. In the case of a solid reagent

particle, the viscous mass transfer rate in the continuous phase surrounding a rigid sphere can be calculated with the Ranz-Marshall correlation: [16]

$$\mathrm{Sh} = \frac{\beta_{[\mathrm{S}]} d_{\mathrm{p}}}{D_{[S]}} = 2 + 0.6(\mathrm{Re})^{\frac{1}{2}}(\mathrm{Sc})^{\frac{1}{3}}, \quad [9]$$

where $D_{[\mathrm{S}]}$ is the reference mass diffusivity of sulfur in the metal phase, Re is the Reynolds number, Sc is the Schmidt number and Sh is the Sherwood number. Based on the limit of the Sherwood-number (Sh = 2 when Re = 0) and the expression of the macrokinetic rate constant, the averaged particle size in terms of a viscous mass-transfer in a diffusion-controlled process can be formulated as: [3]

$$d_{\mathrm{ka}} = \left(\sum_{i=0}^{k} \frac{\% \, Vol, i}{100 d_{p,i}^2} \right)^{-2}, \quad [10]$$

where $\% \, Vol, i$ corresponds to volumetric percentage of particle size class *i* in the differential particle size distribution. The transitory desulfurization reaction is assumed to occur within the ascending trajectory of the reagent particles, during which the injected particles are assumed to reach their terminal velocity very fast. The terminal velocity of a single particle size class was solved from force balance using the drag coefficient correlation proposed by Lapple. [16]

D. *Criteria for particle-metal contact*

In literature, a major factor that to limits the surface area in the injection is presented to be the number of particles that get into contact with the melt, referred as the contact control. [12, 17, 21] Mathematical treatments of the limited contact of fine-grade particles have been employed for calcium carbide[13, 21]. Chiang *et al.* [21] suggested that only 30% of the injected particles get into contact with the melt based on the theoretical expression of desulfurization rate in the plume, whereas Zhao and Irons [13] proposed that the fraction of non-contacted reagent particles can be determined from the heat-balance of the system. Lee and Morita[17] stated that the particles with a diameter less than 100 μm do not necessarily wet the hot metal phase in

full-scale injection due to surface forces of the continuous phase, and may float on the surface unreacted. [17]

In practical injection conditions, the velocity of particle jet in the injection lance is 40% of the gas velocity. [23] The velocity profile of particle-gas flow cannot be considered as uniform as the boundary layer between the individual particles is a function of particle diameter and density.[7] The directional gas-particle-force balance calculations reveal that the terminal velocity of very small size classes approaches 0, and so it is possible that particles move with almost an equal velocity with the gas phase, or at least very close to terminal velocity. In CFD-modeling study of a dephosphorization process with solid lime, the particle jet velocity profile has been discovered to follow a normal distribution.[24] Therefore, in this study the particle velocities in the continuous gas-phase were assumed to follow a normal distribution with an expected value of $0.4u_g$, and a standard deviation derived from the $E(x) \pm 3\sigma$. The velocity of a single particle in the lance tip can be thus treated as a random number drawn from a normal distribution, which is given as:

$$u_p \sim N(E(x), \sigma^2) \sim N\left(0.4u_g, \left(\frac{0.4u_g}{3}\right)^2\right), \quad [11]$$

where $E(x)$ is the expected value for a particle velocity and σ is the standard deviation of velocity. Nakano and Ito [12] gave a quantitative measure for the minimum penetration velocity, which corresponds to a velocity to be exceeded in order for a particle penetrate through gas-metal-interface. This velocity can be expressed as a function of single particle diameter based on a critical Weber number, which is given as: [12]

$$\mathrm{We}_c = \frac{1}{0.044}\left\{\left(1 - exp\left(\frac{0.66}{\rho^* + \frac{1}{4}}\right)\right)\left(\frac{\rho^* + \frac{1}{4}}{0.33} - 1 + \cos\theta\right) + 2\right\}, \quad [12]$$

where We_c is the critical Weber number, θ is the contact angle of solid CaO and hot metal and ρ^* is the relative density between continuous and dispersed phases. The critical penetration velocity can thus be solved from the expression of the critical Weber number as: [12]

$$u_c = \sqrt{\frac{\mathrm{We}_c \gamma}{\frac{d_p}{2}\rho_l}}, \quad [13]$$

where u_c is the critical penetration velocity for a particle size and γ is the surface tension of the continuous phase. Desulfurization reaction between the reagent particles and the hot metal occurs only if the injected particles are wetted by the melt. [17] Therefore, the rate constant for a particle size class that is contact with the hot metal can be expressed by weighting the expression of rate constant with a binary variable Φ. The values of Φ are defined as:

$$\Phi = \begin{cases} 1, & if\ u_p \geq u_c \\ 0, & if\ u_p < u_c \end{cases}. \quad [14]$$

From **Eqs. 11-14**, it results that the probability for reagent-metal contact is proportional to the diameter of the particle size class. This is due to the fact that critical Weber number is both a function of surface tension and diameter of the reagent particle; with constant surface tension a smaller particle size class results as a higher critical penetration velocity, from which follows that the probability for particle-metal contact approaches zero as the diameter of the particle approaches 0. The contact angle between solid particles and hot metal, and the surface tension of hot metal were extracted from the literature. [17]

E. *Injection of gas-releasing agents*

The injection of limestone as a gas-releasing additive within a desulfurization reagent has been studied only in the case of calcium carbide.[5, 25] The injected limestone is assumed to decompose through a following reaction: [19]

$$< \mathrm{CaCO_3} > \rightarrow < \mathrm{CaO} > + \{\mathrm{CO_2}\} \quad [15]$$

In the case of a calcium carbide, the injection of limestone is observed to improve the reaction kinetics by providing more solid surface area for metal-reagent contact, but also to limit the rate of desulfurization due to possibility for the increase of oxygen potential in the system through Boudouard reaction equilibrium. [5, 25] The increase in the solid-surface area by adding gas-releasing agents was later confirmed by Lindström *et al.* [14] for lime-magnesium

reagent mixes. [14] The effect of gas-releasing agents on the mixing of the metal bath was found to be negligible compared to the flow rate of the carrier gas by Irons [5]. Based on the studies conducted by Lindström and Sichen [18], the increase in the oxygen potential of the system leads to more thermodynamically favorable conditions for the formation of $2CaO{\cdot}SiO_2$-product layer, which on the other hand could be prevented by decreasing the particle size of lime. [4, 18] Although, when hot metal desulfurization operates a very far from thermodynamic equilibrium state, the increase in the provided solid surface area assumedly has more prominent effect on the rate of the desulfurization than the oxygen potential, as in the high sulfur concentrations the reaction is controlled by rate of mass transfer and not by the thermodynamic driving force. Also, it is worth mentioning $2CaO{\cdot}SiO_2$ covers only half of the nominal surface area of the injected particles. [6] Nevertheless, the extent to which the injection of gas-releasing agents improves the rate of desulfurization in the industrial scale hot metal desulfurization remains unclear.

As the kinetics of calcium carbonate decomposition is not comprehensively studied in the operational temperature of hot metal desulfurization, the effect of particle size distribution of limestone on the rate of decomposition is ignored from the approach. [19] Similar to Irons [5], the injected limestone particles are assumed to decompose instantly as the reagent particles are introduced to the melt. This assumption is based on the following considerations. First, despite the heat consuming decomposition reaction the heat flux between single limestone particle and the hot metal is large. Second, owing to their small size, the Biot number is estimated to be << 0.1 and consequently, the heat transfer is virtually independent from the internal resistances of the limestone particles. Thus, a simplistic expression for the volume of injected gaseous compound and carrier-gas in hot metal per unit of time is derived from the ideal gas law and can be expressed as follows:

$$Q_{tot} = Q_{\mathrm{N_2}} \frac{p_{inj.}}{(p_{atm} + \rho_{\mathrm{Fe}} g h)} \frac{T}{T_{\mathrm{STP}}} + \frac{\dot{m}_r w_{\mathrm{CaCO_3}} R T}{M_{\mathrm{CaCO_3}} (p_{atm} + \rho_{\mathrm{Fe}} g h)}, \quad [16]$$

where Q_{tot} is total amount of gas in the system per unit of time, $p_{inj.}$ is the pressure of the injection gas, T is the temperature of hot metal, T_{STP} is the temperature in standard conditions, $Q_{\mathrm{N_2}}$ is the flowrate of carrier-gas, $w_{\mathrm{CaCO_3}}$ is the mass-fraction of limestone in the reagent mix,

M_{CaCO_3} is the molar mass of limestone, h is the injection depth, p_{atm} is the atmospheric pressure and g is the gravitational constant.

F. *Parameterized expression for the rate constant*

In the research conducted by Chiang *et al.* [21] and Coudure and Irons [3] the rate constant of desulfurization with a carbide-based reagent was expressed based on operational variables and initial slag condition. It was suggested that the rate constant for transitory desulfurization reaction could be formulated by applying a logistic multivariable regression model of a following multiplicative form: [3, 21]

$$k_{tot} = 10^{b_0} \prod_{i=1}^{n} x_i^{b_i}, \qquad [17]$$

where i is the number of a variable, n is the total number of prediction variables in a regression model and b_i is the corresponding regression coefficient. The original models were derived individually for operational parameters, particle size distribution and initial slag condition, but did not account for their interactions. For this reason, the models proposed by Coudure and Irons[3] and Chiang *et al.*[21] of are far too simplistic to apply in the prediction of high-dimensional industrial problems. In the surface-area based approach, the rate constant is directly proportional on the term $(A/V)_p$, but due to the fact that all of the injected solid surface is not available for extraction and keeping in mind the high complexity of the injection of multiple particles, the increase of the surface area can be assumed to follow a logistic, rather than a linear growth. As there still is a large uncertainty related to the system identification, the relation between the theoretical rate constant and actual rate constant can be assumedly given as:

$$k_{tot} = e^{b_0} k_{tot}^{b_j}, \qquad [18]$$

where b_j is the corresponding regression coefficient and e^{b_0} is the pre-exponential bias-term, which summarizes the effect of unknown process variables on the rate of transitory reaction. It should be noted that if the mathematical description of the rate constant strictly corresponds to the actual process, the values of e^{b_0} and b_j should approach unity, which is rarely true in the case of full-scale processes. Now, the regression coefficient gives the limit of the ratio of the percentage change in the time constant and the percentage change in the input variable. The multiplicative model is suitable especially in the situations where it relates fundamental uncertainties to the measured variables. [31] For instance, if it is considered that there is a certain fraction of particles that gets into contact with the metal phase, but only measurable variable is the particle size distribution and the actual flow rate, the effect of the solid surface-area on the rate constant can be given as:

$$\boldsymbol{A_{Solid}} = \Omega \boldsymbol{A_{injected}}. \quad [19]$$

Where $\boldsymbol{A_{Solid}}$ is the actual solid surface area and $\boldsymbol{A_{injected}}$ is the injected surface area. Now $\boldsymbol{\Omega}$, denoting the fraction of particles that get into contact with hot metal, is an unobservable variable. From the form of the rate constant it results that the error term in the multiplicative prediction model is a function of corresponding regression coefficient:

$$\boldsymbol{\varepsilon} = \Omega^{-\boldsymbol{b_j}} \quad [20]$$

And furthermore for the whole expression of rate constant, the error term can be given as:

$$\boldsymbol{\varepsilon_i} = \prod_{\boldsymbol{j=1}}^{\boldsymbol{k}} \Omega_{\boldsymbol{ij}}^{-\boldsymbol{b_j}}, \quad [21]$$

where $\boldsymbol{\Omega}$ is the unknown factor related to each of the variables in the expression of rate constant, in example the residence time, mass-transfer coefficient and the contact ratio. Thus, when writing the multiplicative form of the model, the product of measurable variables and unknown factor are absorbed into the pre-exponential bias-term, and the error of the prediction is a function of the unknown factors. [31] Keeping in mind the aforementioned

assumptions of, the surface-area approximation based rate constant for a single size-class can be expressed in a multiplicative form:

$$k_{tot} = e^{b_0} \left(\frac{6}{d_\mathrm{p}}\right)^{b_1} Q_{tot}^{b_2} \left(\frac{\dot{m}_r}{\rho_r}\right)^{b_3} \left(\frac{\rho_\mathrm{Fe}}{m_\mathrm{Fe}}\right)^{b_4} \varepsilon. \quad [22]$$

III. MODEL PARAMETER IDENTIFICATION

The identification of the parameter vector to predict the rate constant was carried out based on two types of least-squares cost-functions; linear and non-linear. In the linear case, the end sulfur content was predicted based on the predicted rate constant. The analysis of experimental data was carried out with multivariable regression (MLR) modeling. The MLR-model is capable of revealing the magnitude and direction of interaction of the selected input variables to the output variable, and so can be applied to the analysis of the data and to selection of set of explanatory variables that explain the majority of variance of the output vector. In the analysis of the MLR-model outcome, two possible hypotheses for interactions between explanatory and output variables can be stated: [8]

- H_0 – Null-hypothesis; the selected explanatory variable does not explain the changes in the output variable ($b_j = 0$).
- H_α – Alternative hypothesis; the selected explanatory variable explains the changes in the output variable ($b_j \neq 0$).

The effect of explanatory variable x_i on the outcome is interpretable from the value of the corresponding modeling coefficient b_i. A linear form of multivariable regression model can be expressed as a sum of weighted interactions of linearly independent explanatory variables as follows: [8]

$$\hat{y} = b_0 + b_1 x_1 + \cdots b_j x_j = b_0 + \sum_{i=0}^{j} b_i x_i + \varepsilon, \qquad [23]$$

where $\hat{y}$ is the output variable or the dependent variable, x_i is the independent explanatory variable and b_i is the regression coefficient, b_0 is the intercept, j is the number of variables in the prediction model and ε is the error term. The **Eq. 23** is applicable for prediction if and only if the sum of weighted interactions follow linear relationships between the predicted output and explanatory variables. In the case of complex process dynamics, the relationships are hardly ever linear, due to the fact that chemical reactions rarely follow zero-order kinetics.

Therefore, a multiplicative form of a regression model is assumedly more applicable approach, which can be formulated as a multivariable linear regression model: [31]

$$\ln \hat{y} = b_0 \ln e^1 + b_1 \ln x_1 + \cdots b_n \ln x_n = b_0 \ln e^1 + \sum_{i=0}^{j} b_i \ln x_i + \varepsilon, \quad [24]$$

where y_i is the measured outcome. The multivariable linear regression model can be written in a matrix form: [8]

$$\hat{y}_i = \mathrm{Xb} + \varepsilon, \quad [25]$$

where X is the matrix containing the input vectors and b is the vector for regression coefficients. The input vectors in the matrix X constitute of the measurement data of independent variables. The linear independency of the design matrix can be determined by calculating *rank*(X). For a full rank, *rank*(X) = *j*+1, which is a sufficient criteria to establish the design matrix to be linearly independent. The regression coefficients are obtained by solving a least squares optimization problem, in which the objective function is formulated as: [27]

$$\min \sum_{i=0}^{M} (y_i - \hat{y}_i)^2, \quad [26]$$

where M is the number of outcomes. In optimization the formulation of a proper objective function is essential in order to acquire reasonable results for the parameter vector *b*. In the identification of the empirical weight coefficients, a linear cost-function can be considered:

$$\mathbf{min} \sum_{i=1}^{M} \left(k_{tot,i} - e^{b_0} \left(\frac{6}{d_{ka,i}} \right)^{b_1} Q_{tot,i}^{b_2} \left(\frac{\dot{m}_{r,i}}{\rho_r} \right)^{b_3} \left(\frac{\rho_{\mathrm{Fe}}}{m_{\mathrm{Fe,i}}} \right)^{b_4} \right)^2. \quad [27]$$

The form of the prediction equation can be converted into a linear form, and thus be expressed as follows:

$$\ln k_{tot} = b_0 \ln e^1 + b_1 \ln \frac{6}{d_p} + b_2 \ln Q_{\mathrm{tot}} + b_3 \ln \frac{\dot{m}_r}{\rho_r} + b_4 \ln \frac{\rho_{\mathrm{Fe}}}{m_{\mathrm{Fe}}}. \quad [28]$$

Now the problem is to find a solution for the vector $b = [\boldsymbol{b_0}\ \boldsymbol{b_1}\ \boldsymbol{b_2}\ \boldsymbol{b_3}\ \boldsymbol{b_4}]$, which gives an appropriate least-squares approximation of the system dynamics and succeeds to describe the changes in the output-variables ($\boldsymbol{k_{tot}}$ and $[\mathbf{S}]$) with reasonable accuracy. It can be shown that the least-squares solution for a linear parameter identification problem can be given as the product of pseudoinverse of matrix X and the output vector *y* as: [8]

$$\mathrm{b} = (\mathrm{X}^T\mathrm{X})^{-1}\mathrm{X}^T y. \qquad [29]$$

It should be noted that the b_0 for a regression model is obtained by inserting a vector of ones for the corresponding column of X with respect to b-vector. The main problem of the linear formulation is that the solution for the weighted time constant could be strongly biased such that the predictions for the end sulfur content can reach irregularly low values if the fitting data contains observations with extremely low sulfur concentrations. The aforementioned problem can be solved by formulating a non-linear form of a cost-function such that the analytical solution of the dynamic sulfur concentration approaches the observed values of end sulfur as a function of time. The objective function can then be expressed as:

$$\mathbf{min} \sum_{\boldsymbol{i=0}}^{\boldsymbol{M}} \left([\mathbf{S}]_{t,i} - [\left([\mathbf{S}]_{0,i} - [\mathbf{S}]_{\mathbf{eq}}\right) \boldsymbol{e}^{\left(-\left(e^{b_0}\left(\frac{6}{d_{p,i}}\right)^{b_1} Q_{tot,i}^{b_2}\left(\frac{\dot{m}_{r,i}}{\rho_r}\right)^{b_3}\left(\frac{\rho_{\mathrm{Fe}}}{m_{\mathrm{Fe,i}}}\right)^{b_4}\right)t\right)} + [\mathbf{S}]_{\mathbf{eq}}] \right)^{\mathbf{2}}. \qquad [30]$$

It is observable from the form of **Eq. 30** that the cost-function is non-convertible into a linear form. For this reason, the parameter vector *b* has to be solved numerically. For this task, a suitable numerical solution strategy is considered. While examining form of the non-linear cost-function and inspection of the data, it can be seen that as the sulfur contents in the hot metal are in ppm-level, a local optima for a least-squares solution is $\hat{\boldsymbol{y}} = \overrightarrow{[\mathbf{S}]_{\boldsymbol{eq.}}}$, which is the steady-state solution of the mass-transfer controlled desulfurization reaction. The aforementioned solution can be found with very high values of the modeling coefficients $b_1 \ldots b_4$, if the b_0 is in physically relevant order of magnitude. This makes it evident that the efficiency of the iterative search is highly dependent on the initial value of *b*.

A. *Genetic algorithm*

To obtain the least-squares solution for the non-linear cost function, a genetic algorithm (GA) was applied. GA belongs to the family of evolutionary search methods, as it mimics the natural selection in the iterative process.[49] GA is a robust numerical solution strategy, which has been applied successfully to multivariable optimization and parameter identification problems in various fields, including metallurgy, signal processing, electrical engineering, energy systems, hydrodynamics, automation engineering, and many more. [28, 29, 32-36, 38, 40, 47, 48, 50]

GA can be implemented with various structures. A simple genetic algorithm is composed of three basic operators: reproduction, crossover and mutation. [49] The nature of the problem defines the suitable combination of different genetic operations, some of which performance is dependent on the computational parameters, ergo size of the population, maximum number of generations, crossover probability and mutation probability. [32-36, 48, 49] In this study, a non-adaptive GA was applied, which means that the computational parameters are selected manually based on trial and error procedure by applying some rules of thumb summarized in the literature.

In this study, a binary coded genetic algorithm was applied. The initial population is generated by tossing a non-biased coin, ergo generating a random number between 0 and 1 following a uniform distribution. [49] If the random number is smaller than 0.5, the bit is assigned with 0, and with 1 otherwise. A chromosome population constitutes of parameter vectors b coded in binary digits such that each member of a population is a $l \; x \; k$+1 – dimensional matrix, where l is the number of binary digits in a single chromosomes and k is the number of variables and the bias-term. The first digit of the chromosome determines whether the chromosome is assigned with a negative value; if the first digit is equal to one, then the chromosome is coded negative.

The task of selecting a suitable population size is highly dependent on the system under study.[51] If the target system is high dimensional or otherwise complex, a large population often gives more desirable results than a small population. However, an excessively large

population demands higher computational resources and does not necessarily provide a higher accuracy [50], and in some cases can result even as deteriorated performance of the algorithm. [51] Consequently, a feasible size of the population is to some extent a compromise between the computational resources and the desired accuracy.

The convergence of a population towards the solution of the problem is achieved with a crossover. In this study, a single-point crossover was applied. The basic idea of a crossover is that two selected parent chromosomes produce two offspring chromosomes. The reproduction of a new individual is conducted by swapping n number of bits between the parent chromosomes. In a single-point crossover, the number of bits swapped is $n = l - r$, where r is the randomly selected crossover point. The rate of crossover is regulated with a crossover probability. The crossover is performed if the random number between 0 and 1, generated from a uniform distribution is below the crossover probability. Otherwise, the individuals are moved to the next generation. [49]

The selection of an individual for crossover is based on the roulette-wheel selection, in which the probability for an individual to be selected is directly proportional to its fitness. [49] In a minimization problem, the evaluation of fitness of the individuals is based on the inverse of the objective function. To avoid the convergence towards the steady-state solution, the aforementioned is combined with a penalty condition. The penalty condition is a simple scaling, in which the fitness of the individual is reduced, as proposed by Goldberg [49]. As was proposed by Gharahbagh and Abolghasemi [42], the number of parents selected to produce a new offspring is $n_{pop}/2$. [42] The penalty is given for a member of a population if the predicted end sulfur content is below the thermodynamic equilibrium content.

Similar to e.g. Sattarpour *et al.* [41], the mutation operator is implemented after the crossover, but such that every gene of a selected individual are treated by a bitwise inversion with a certain mutation probability. [42] Even though the mutation operator is considered as a secondary operator in a genetic algorithm, the mutation often leads more reliable convergence towards the extreme of the objective function, which can be further associated to increased diversity of the generations. [49] The suitable value for mutation probability is dependent on both the properties of the individuals and the formulated problem. For example some studies have achieved good results with low mutation rates $p_{mut} = 0.01$ [36], and in some studies a

mutation probability as high as p_{mut} = 0.8 [32] is applied successfully in parameter identification.

Bäck and Schütz [48] studied different control mechanisms for a mutation probability. In their study, it was established that a deterministic mutation rate schedule gives desirable results for convergence. [48] Although, when inspecting the limit of the deterministic schedule proposed by the authors it is seen that the limit for the rate of mutation is dependent on the length of the chromosome, hence $\boldsymbol{p_{mut}(T-1) = l^{-1}}$ [48], which results that the rate of mutation is relatively large during the last generations with a small length of a chromosome, which could cause a loss of valuable information. This being so, in this study the rate of mutation proposed by Bäck and Schütz [48] is modified such that $p_{mut} \rightarrow 0$, when $k \rightarrow \boldsymbol{T}$. Thus, the mutation probability is given by:

$$\boldsymbol{p_{mut}(k) = \left(2 + \frac{l-2}{T-1}k\right)^{-1} - l^{-1}}, \quad [31]$$

where $\boldsymbol{p_{mut}}$ is the mutation probability, k is the generation, n is the length of the chromosome and T is the maximum number of generations. The chosen structure of the genetic algorithm for this study is illustrated in **Figure 1.**

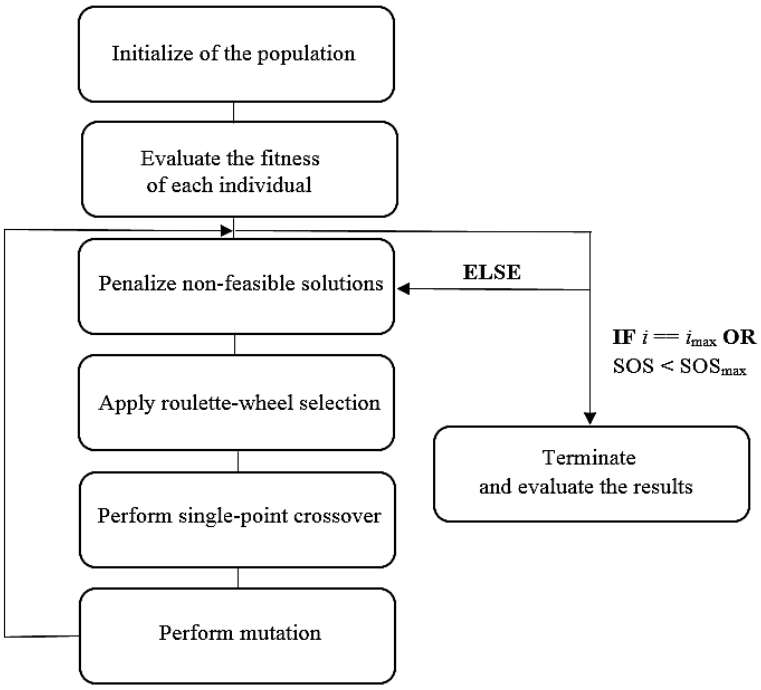

Fig. 1 – Structure of the implemented algorithm.

B. *Nelder-Mead algorithm*

The Nelder-Mead algorithm is a computational algorithm, which is suitable for minimizing a non-linear multivariable cost-function.[45] Nelder-Mead falls under a category of direct search methods as the implementation does not require a knowledge of the objective function derivatives. [43] Nelder-Mead is often claimed to be robust for noisy or discontinuous objective functions, and thus it is widely popular in several fields of research. [39] In various studies, Nelder-Mead algorithm is successfully applied for solving multivariable optimization problems. [39, 40, 43-46] The principal idea of the Nelder-Mead algorithm is based on the adaptive simplex, of which number of dimensions corresponds to j+1. In this study, a commercial Nelder-Mead algorithm (Matlab: fminsearch) [46] was applied to evaluate the consistency of the results provided by the GA, and thus a more detailed description of the algorithm and its convergence properties is provided in the literature.[44,45]

C. *Evaluation of fit*

The evaluation of the solution vector provided by a parameter identifying strategy often demands external knowledge of the system functioning and an external validation of the obtained type of the model. For example, the best solution found based on the fitting data is not necessarily the physically most feasible solution, as it is rather typical that the data is over-fitted. This is often faced when the prediction model contains an excessively large number of variables compared to observations, or when the data set is noisy or collinear.

The cross-validation process is mandatory especially in preventing the over fit of the data. The cross-validation process consists of two parts; fitting and external validation, also referred as testing. When there are multiple set of parameters that produce almost an identical outcome for the minimization problem, the evaluation of the model performance is recommended to be conducted with cross-validation. [37] Thus, it is obvious that a reliable result is the one that explains the variance both in the fitting and external validation data. Prior to fit, the applied

data-set is split such that the data applied in the external validation contains no data that is applied in the fit a priori to external validation. In this study, 67.5% of the data was applied to fit and 32.5% for external validation. A flowchart of the cross-validation process is shown in **Figure 2.**

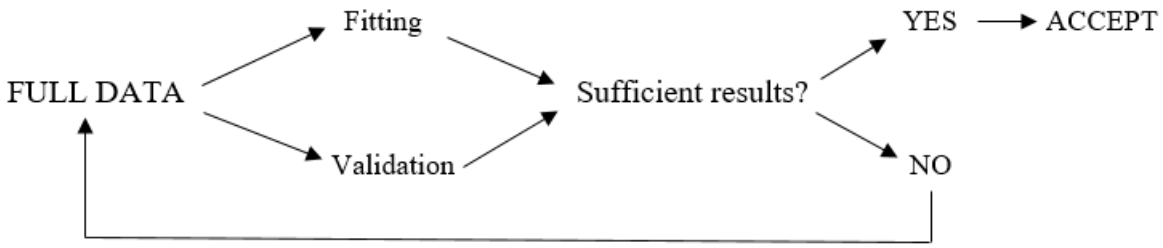

Fig. 2 – Flowchart of the cross-validation process.

The performance of the prediction models was evaluated to obtain a quantitative measure for the prediction accuracy for each of the model types. Evaluation of the statistical significance of the prediction models was based on two-tailed *t*-test, analysis of *p*-value as reported in [10, 30], coefficient of determination (R^2), sum of squared error (SOS) and mean absolute error of prediction (MAE). The linear interaction between the measured input and output can be quantified by the so-called Pearson correlation coefficient (R). The correlation coefficient describes the linear dependency between the two variables. The value of the correlation coefficient varies between -1 and 1, of which $R = -1$ indicates perfect inverse linear dependency and $R = 1$ indicates perfect linear dependency. The square of the correlation coefficient R^2 measures the percentage of the output variable variation, which can be explained by the fitted MLR model. [31]

IV. EXPERIMENTAL DATA

The experiments at the desulfurization site were carried out by applying five lime-based desulfurization reagents with varying particle size distributions and amounts of limestone in the reagent mix. The experiments were conducted in 80 t ladles with an average processing time of 8 minutes. The average hot metal composition at the primary hot metal desulfurization site is C = 4.5 wt-%, Si = 0.45 wt-%, S = 0.045 wt-% and Mn = 0.172 wt-%, whereas the average temperature is around 1623 K (1350 °C**)**.The particle size distributions for the reagents were determined prior to experiments by laser-diffraction analysis. The volume-based characteristic particle size distributions of lime mixed with the limestone, with corresponding average diameters based volume, surface area and formulation based on the mass-transfer law are presented in **Table I**. It should be noted that the particle size distribution of the limestone was approximately constant during the experiments.

The analysis of the hot metal samples was carried out by C-S-combustion method and by X-Ray Fluorescence (XRF). The hot metal samples were taken instantly before and after desulfurization treatments to obtain a representable set of samples, and to minimize the effect of sulfur pick-up assumedly originating from the inverse permanent contact reaction. During the injections, the carrier gas flow rate and immersion depth of the injection lance were held constant, which is why the value of Q_{tot} can be considered as a pure function of temperature and injection rate of limestone at constant pressure. The data-set consists of 40 data-points overall. The full data-set is presented in **Table II**.

V. RESULTS AND DISCUSSION

The calculations based on the theoretical expression for the rate constant were carried out prior to variable selection for the parameterized prediction models. The predictions were conducted by applying different expressions for a reagent particle size distribution. To inspect in what extend does the gas-forming additives increase the predictive power of the theoretical model, the corresponding regression coefficient was identified by applying MLR.

A. *System identification and variable selection*

According to the results of the simulations, the variables, which explain a majority of variance of the desulfurization kinetics are the particle size distribution, mass flow rate of the reagent, carrier-gas flow rate and mass of the hot metal. This is in consistence with the principal component analysis, which reveals that 92 % of the variance in the data can be captured within four principal components. The design matrix determined for such set of explanatory variables full-fills the presumed criteria for linear independency, as the rank(X) = 5. The criteria for independency is full-filled due to the fact that the amount of $CaCO_3$ mixed within the reagent varies between the experiments. Thus, the particle size distribution, the mass flow rate and the total gas flow rate can be applied in the predictions without the problem of multicollinearity.

The surface area-based approximation presents that when applying an extensively fine-grade particle size distribution, the average residence times to achieve a decent prediction accuracy are relatively short. Also as the model assumes that the thermodynamic extraction capacity of a single size class is practically infinite, which thus ignores the solid-state diffusion controlled phase. The surface-area approximation also ignores the fact that as a single particle is in equilibrium with the melt, there are no advantages achievable with longer residence times. For this reason, the predictions conducted with a surface area approximation tend to reach the state of thermodynamic equilibrium, which is in practice non-achievable with decent material consumption.

A major factor that increases the prediction accuracy of the model is the defined criteria for particle-metal-control. In example when comparing the reagents B and E, it is observable from the simulation results that the finer gradation results in approximately 10 %-point drop

in the fraction of particles that get into contact with the metal phase. This is due to the fact that Weber number is both a function of surface tension and diameter of the penetrated particle. The smaller particle size class results as a higher minimum penetration velocity, and so the probability for particle contact is smaller, but highly dependent on the expected value of a single particle velocity at the tip of the lance. The result is in qualitative accordance with the results obtained by Jin *et al.* [26], although they employed a coarser particle size distribution in the simulations, which resulted in a larger number of contacted particles. [26]

The calculations suggest that in order to maximize the desulfurization efficiency of the reagent, the particle size of lime cannot be decreased endlessly. In the case of a full particle size distribution, the existence of particles with a very low contact probability potentially decreases the extraction capacity of the overall distribution. The predictions show that the non-contacted reagent fraction can be compensated with a finer gradation, because the extraction capacity for a fine-grade reagent particle size-class is significantly higher than the corresponding value for coarse size-classes. The aforementioned factors indicate that rate constant cannot be linearly dependent on the mass flow rate and reciprocal of the particle diameter, but should rather follow a logistic growth, and also that the corresponding modeling coefficients for the variables should be smaller than 1 in the case of operational variables.

B. *A static approach in parameter identification*

Based on the whole data, the MLR-model that explains a majority of variance in the stoichiometric yield of the injected reagent can be expressed as a linear combination of four explanatory variables; Henrian activity of sulfur, particle size distribution parameter d_{80}, amount of limestone in the reagent mix and the measured mass-flow rate of the reagent. The variables were chosen with a forward-selection procedure. The Henrian activity of sulfur was calculated based on WLE-formalism, for which the interaction coefficients were extracted from the literature. [20] The predictive power of the model can be considered relatively accurate, even though the gathered data-set is relatively small. This is due to the fact that the coefficient of determination gives a high value (R^2 = 0.92) and the averaged absolute prediction error is small (MAE = 0.5). In the test-statistic point of view, the variables selected in the prediction model explain the changes of the stoichiometric efficiency, as the quantitative measure of evidence against acceptation of null hypothesis is in order of magnitude of 10^{-4}-10^{-16}, which fulfills the presumed criteria for the p-value < 0.01.

The coefficient of determination for the whole data set is R^2 = 0.94. When inspecting the reliability factors for independent predictors it can be clearly seen that selected set of variables gives statistically significant results due to the fact that the probability to make a false interpretation based on the regression coefficient is very low, which can be deduced from the fact that *p*-value is significantly lower than the stated confidence level. However, it can be interpreted that the desulfurization efficiency and the stoichiometric yield of the reagent described well with simple linear interactions only within a certain operational area. Based on the values of the regression coefficients, it can be interpreted that the stoichiometric yield of the injected reagent can be increased by increasing the activity of sulfur in the hot metal before the treatment, applying a finer-grade reagent and by injecting gas-forming additives within the lime. Based on the statistical prediction, by decreasing the mass flow rate of the reagent, which results as an increased treatment time and decreased solid/gas load with a constant carrier gas flow rate, the yield of the reagent can be improved.

The more detailed analysis of the model reveals that the solid surface area in the reaction system potentially controls the material efficiency of the process, as the reagent yield has a dependency on both particle size distribution and injected amount of limestone. This is due to the fact that the surface area provided by the injected material is inversely proportional to single particle diameter. However, the static prediction model is applicable only in limited number of cases, as the molar efficiency of solid CaO follows the 1st order kinetics. Therefore, the regression coefficients are highly a function of target sulfur content, which practically rules out the possibility of applying static linear prediction models for hot metal desulfurization, which is further confirmed as a poor predictive power of the model for end sulfur content. It is also reported in the literature that the MLR method fails in the parameter identification problem, when the applied data for the fit is noisy or collinear. However, the static approach identifies the most significant single factors, and thus creates a baseline for the further inspection of dynamic model forms.

C. *Parameter identification for dynamic models*

The identified modeling coefficients for 67.5% of the data are presented in **Table III.** An illustration of the fit is provided in **Figure 3**. It can be seen that all of the identifying methods give reasonably consistent results for the model parameters, especially in view of the effect of

particle size distribution on the rate constant. It is also evident from **Figure 3** that the solved coefficients are capable of predicting changes in the sulfur content based on the fitting data with sufficient accuracy. The main uncertainty is related to the cross-correlation of the exponential bias term b_0 and to the coefficient related to the volume of the hot metal phase. Nevertheless, all of the fitted bias terms are in accordance with the theoretical considerations as it is expected that $t_{res}\beta_{[S]} < 1$ even with relatively long residence times. It is worth noticing that the actual values of mass transfer coefficient and the residence time of single size class are collinear, as both of the variables are a function of particle Reynolds number through the ascending velocity of the particles in the hot metal. The dynamic model proposed for the rate of desulfurization agrees well with the static reagent efficiency model. Unlike in the case of static linear model, the evolution of stoichiometric yield and desulfurization efficiency are actually a function of sulfur concentration gradient, which implies the time dependency of the aforementioned model. This indicates that a linearized static model formulation, which apply the stoichiometric yield, or the desulfurization efficiency as dependent variables are not applicable for predicting the end sulfur content as precisely as a dynamic non-linear approach.

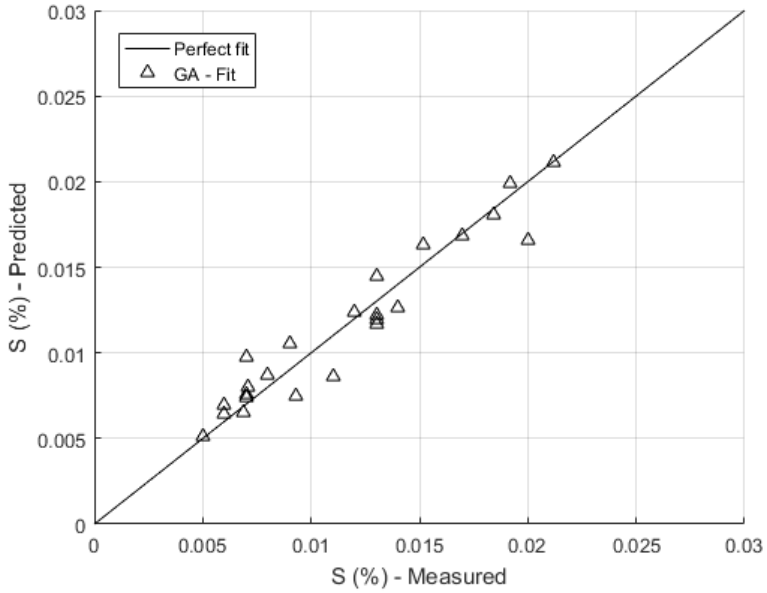

Fig. 3 – Prediction results for the fitting data. Model parameters are identified with GA.

D. *Analysis of the modeling results*

The prediction error of the surface area approximation can be drastically improved by applying the RRS distribution and the derived contact criteria. Applying a full particle size distribution does not provide any additional benefits compared to a single particle model, apart from a slightly smaller average error of prediction. The prediction ability of the surface area approximation is drastically increased when the limited contact criteria and the effect of gas-forming compounds identified with MLR is added to formulation of the rate constant.

In **Table IV**, the modeling results are summarized for each of the studied model types. The surface area approximation was found to predict too high desulphurization rates; this is highlighted by the fact that in many cases the sulfur content reached its equilibrium value. It can be seen that the surface area approximation provides accurate results in a few of the cases, and in the others the results are merely suggestive.

Nevertheless, the parameterized expression of the rate constant gives more accurate results regardless of the method of identifying the parameters. The result can be explained well by the fact that the effective surface area in hot metal desulfurization differs significantly from the nominal surface area of the particles. This is mainly due to the fact that the surface area approximation does not take the internal mass-transfer resistances of the lime particles into account, and so gives adequate results only in limited cases.

In the case of the parameterized solutions, the effect of particle size distribution on the rate of desulfurization is obvious: a finer particle size distribution improves the reaction kinetics. However, the accuracy of the parametrized rate constant is on some extend dependent on the applied distribution parameter. For example, when solving the coefficient vector b by applying the mass transfer averaged mean diameter, the formulated model tends to underestimate the model coefficient related to surface area, although the corresponding modeling coefficient is in the same order of magnitude ($b_1 \approx 0.5$) as in the case of distribution parameter $d_{80.}$ This is interpretable from **Table I** and from the differential particle size distribution of reagent D, which contains a relatively large volume fraction of particles with a diameter less than 1 µm. The contact probability of the particles of such a small size class is very low, and so both the surface area and mass transfer averaged diameters do not properly

describe the changes in the effective solid surface area (A_{solid}) in **Eqs. 19** and **22**, as the theoretical surface area differs significantly from the nominal surface area of the particles.

Eq. 22 suggests that, for instance, in the case of surface area term, the effect of particle size distribution is inversely proportional to the rate constant, but the order of magnitude is dependent on the parameter b_1. In practice this implies that the interfacial area for the reaction can be increased by decreasing the average particle size, but the certain phenomena, namely the limited extraction capacity and residence time of a single particle and the fraction of particles that get into contact with the melt can potentially limit the rate constant. For example, decreasing the d_{80} particle size from 250 µm to 70 µm increases the rate constant by 0.13 1/min (between 30 and 50% depending on the gas flow rate), but as the corresponding regression coefficient $b_1 << 1$, it is evident that the whole injected solid surface area is not used in the extraction of sulfur. In view of the reasoning above, and of earlier studies on the subject,[1, 3, 18] this result can be partially explained with the combined effect internal mass transfer resistances, and thus by limited extraction capacity, and by the formation of $2CaO{\cdot}SiO_2$, which prevents the diffusion of S^{2-} and Ca^{2+} ions to the core of a single particle. It should be noted that the formulation of the multiplicative model form presented in Section **II.F** also concerns the fraction of entrapped particles such that regression coefficients $b_1 \ldots b_3$ are in fact in some extend a function of the contribution of these particles on the overall kinetics. These considerations highlight the significance of the accurate determination of the particle size distribution for the prediction of transitory reaction kinetics.

The effect of surface area on the system kinetics becomes evident from the values of the coefficients b_2 and b_3. On the other hand, the injection of gas-forming compounds assumedly spreads the particles more efficiently to the melt ($b_3 > 0$), or can contribute on the scattering of large carrier gas bubbles in the smaller swarms of bubbles, rather than by increasing the stirring of the hot metal bath. This finding and deduction are somewhat consistent with the results provided by Irons [5] and Lindström *et al.* [14] As the studied process operates very far from thermodynamic equilibrium, it is reasonable to assume that the reduce in the thermodynamic driving force due to formation of CO_2 is negligible.

If the flow rate is increased by 10 kg/min, the time constant is increased by a magnitude of 0.03 1/min, which is between 15 and 30% depending on the gas flow rate. The rate of change in the rate constant due to the change in the mass flow rate is slightly above the theoretical

value of the rate of change, because by increasing the mass flow rate, the flow rate of the gaseous compounds increases as the limestone is mixed within the lime. However, the rate of change of the rate constant decreases within the increase of the mass flow rate, which results as that for excessively high flow rates no additional benefits are achieved by increasing the flow rate of the reagent. Due to the increase in the mass flow rate, the material efficiency of the reagent decreases due to the fact that the concentration gradient acts as the main driving force for a mass transfer controlled reaction. The effect of mass of the hot metal is further discussed in the next section.

The volumetric amount of reagent particles injected in the melt is found to be a less significant factor than the particle size distribution, although the two factors are interrelated, are related also to the total flow rate of the gaseous compounds. Nonetheless, the kinetics of desulfurization seem to be directly proportional to the mass flow rate, although the rate of change in the effect of mass flow rate decreases while increasing the flow rate to excessively high values. This is due to the fact that with high sulfur concentrations, the overall rate of reaction is limited by the solid-state diffusion controlled phase. The kinetics can be further improved by introducing fresh reaction surface to the melt, but at a certain point the solid/gas load can affect to penetration behavior of particles and to carrier gas momentum, which contributes to proper spread of the particles to the metal phase. The model formulation and the solved coefficients are thus in agreement with the earlier studies. [1, 7, 9]

E. *External validation and sensitivity analysis of the dynamic parameterized models*

The external validation was carried out by predicting the end sulfur contents by applying 32.5% of the original data set. The external validation data set was chosen randomly such that it contains at least 3 data points for each of reagents A–E. The external validation results are presented in **Table V.** It can be seen in the table that GA gives the best modeling results based on the cross-validation process. It is seen that MLR and the Nelder-Mead algorithm provide equally good results for the fitting data, as does the genetic algorithm, but it is evident that the parameters obtained with these strategies do not explain the changes in the external validation data as well as does the solution of the GA.

Although MLR and GA provide results with equivalent statistical accuracy, the parameters identified with MLR are not physically feasible. This is interpretable from the coefficient

corresponding to the mass of the hot metal. MLR suggests that $b_4 < 1$, which practically means that the molar efficiency of the reagent increases within the mass of the hot metal. This result is physically irrelevant for two reasons. First, the increased residence time resulting from the increased height of the metal bath does not provide a further increase in material efficiency after the reagent particles are in equilibrium with the hot metal. Second, the relative variation in the height of the metal bath is rather low in typical operation.

The results of the external validation of the parameters obtained with GA are presented in **Figure 4.** The validation result can be considered sufficient as the residuals are equally spread within the diagonal line. Both the coefficient of determination for the fit and external validation is high, R^2 = 0.91 and R^2 = 0.91, respectively. The mean absolute prediction error of the end sulfur content is very small (MAE = 0.0010-0.0012 [wt-%]), which can be considered sufficient in view of the measurement error of the C-S-analyzing device (0–5 ppm).

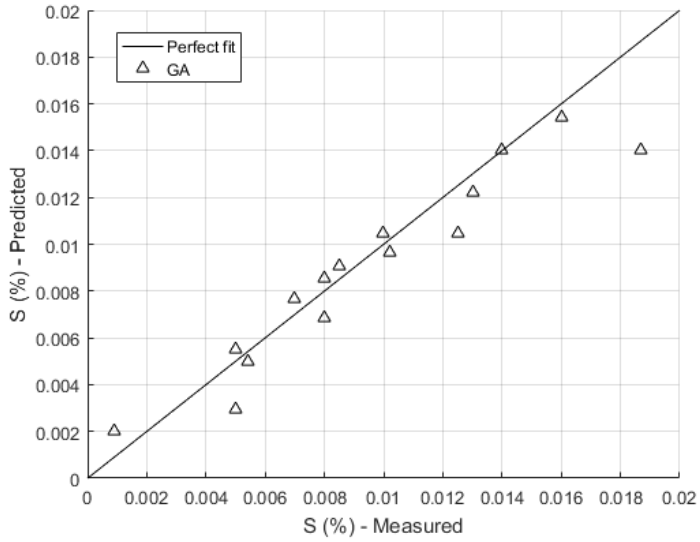

Fig. 4 – Prediction results for the external validation data. Model parameters are identified with GA.

However, the external validation results are highly dependent on the size of the population; typically a small population tends to find a feasible accuracy for the fit, but the solution does not explain well the changes in the external validation data. This is mainly due to the fact that the initialization of the small population does not contain initial guesses with significantly high fitness values with very high probability, and thus the algorithm tends to converge towards a weak solution. A notable difference between the numerical solution strategies is

that unlike the GA, the Nelder-Mead tends to converge towards the steady-state solution. Thus, it is evident that the penalty condition is fundamental to ensure a physically feasible solution under the conditions of this study.

As for the GA approach, the computationally optimal convergence and the best results were achieved with a population size of 200 individuals. Although the number of individuals is high, it has to be noted that the optimization problem is complex in nature, as there are a numerous pseudo-feasible solutions for the parameter vector *b*, which on the other hand provide excessively good results for the fit but fail to predict the changes in the external validation data. This finding is in a qualitative accordance with Deo and Srivastava [48]. Based on the results of the sensitivity analysis and external validation, it can be said that GA, in which the mutation probability follows a deterministic schedule, is a suitable numerical solution strategy for parameter identification. However, the results provided by the GA need to be validated with an external data set and the identification process has to be repeated for a number of times for sufficient results.

Generally, while comparing the results of the fitting and validation process it is observable that the genetic algorithm tends to over fit the coefficients for the data, which results as a poor external validation result. Still, the GA tends to find the solution for the problem with significantly higher probability than the other identification methods applied in the study. For an excessively large search space, the algorithm does not obtain feasible results in decent amount of iterations, and thus the search space is necessary to be constrained such that b_j = [-4 4].

The calculation time for one iteration loop of GA is in order of 0.01 seconds. For a sufficient convergence, the maximum calculation time for a single parameter identification trial is in order of 30 seconds, but is highly dependent on the success of the initialization, desired accuracy and the maximum number of iterations. The initialization can be further improved by applying a non-random initial guesses. In the case of the GA the solution can be found in approximately 15–30 iterations, which corresponds to 0.15–0.3 seconds of computational time. Unlike the commercial Nelder-Mead, the GA identifies the parameters with sufficient accuracy with a high probability. The performance of both algorithms was evaluated based on 500 repetitions. In the case of a GA, a decent accuracy for both fit and validation is achieved with a probabilities of $P(R^2 \geq 0.85) = 0.58$ and $P(\mathrm{MAE} \leq 0.0016) = 0.82$, whereas the

corresponding values for the Nelder-Mead algorithm are P($R^2 \geq 0.85$) = 0 and P(MAE $\leq$ $0.0016) = 0.39$. The summary of the test statistics is presented in **Table VI.**

VI. CONCLUSIONS

The main findings of this study can be summarized as follows:

1) The prediction accuracy of the surface area approximation can be increased by substituting the mass-transfer coefficient and the average residence time of the particles with a pre-exponential bias term. The parameterized approach for the rate constant provides the most accurate results in the viewpoint of process control purposes.

2) The accurate determination of solid surface area and the volumetric amount of injected reagent increase the predictive power of all model types. Without adequate information of the reagent properties and the injection parameters, the accurate prediction of the hot metal desulfurization kinetics is not possible. The analysis also reveals that the effective surface area of the transitory reaction differs greatly from the nominal surface area of injected particles. Based on the results it can be said that applying a finer grade particle size distribution of lime in the injection can be realized in increased reaction kinetics, but certain phenomena, namely the fraction of non-contacted particles limit the reaction kinetics in case of excessively fine-grade particles. However, there is no quantitative measure of the minimum particle size in the injection, even though the probability for reagent metal contact decreases when applying an excessively fine-grade particle size distribution.

3) A non-linear form of a cost function provides physically relevant results, provided that the employed numerical solution strategy is sufficiently robust. The best external validation results are also acquired by applying the evolutionary search method. Under conditions of this study, a modified genetic algorithm is a feasible alternative for parameter identification.

4) When the hot metal desulfurization operates far away from thermodynamic equilibrium, the kinetics of the transitory reaction improved by adding limestone within the reagent. The effect of limestone could be attributed to increased effective solid surface area by scattering of the reagent particles due to gas-forming decomposition reaction.

5) By optimizing the mass flow rate of the reagent, the total consumption of the reagent can be decreased, if the rate constant is of feasible order of magnitude. The decrease in the material consumption is associated with the thermodynamic driving force. It appears that there is an optimum time instant *t* at which the flow rate should be decreased to minimize the overall costs of injection. The cost wise optimization of the injection trajectory demands additional research.

ACKNOWLEDGMENTS

This work was conducted within the Flexible and Adaptive Operations in Metal Production (FLEX) research program funded by Business Finland. The authors would like to thank Dr. Aki Sorsa for constructive comments on the manuscript. Also, the work of the analysis laboratory and specialized sampling group of SSAB Europe Oy in Raahe is greatly appreciated.

NOMENCLATURE

SYMBOLS AND ABBREVIATIONS

A	Area	m^2
b_i	Regression coefficient for a variable *i*	-
C_d	Drag coefficient	-
d	Diameter	µm
d_{ka}	Average particle size by means of mass-transfer	µm
d_{32}	Sauter mean diameter	µm
d_A	Area-based mean diameter	µm
d_{mean}	Volume-based mean diameter	µm
g	Gas	-
k_{tot}	Rate constant of the transitory reaction	1/s
M	Molar mass	g/mol
$\dot{m}$	Reagent feed rate	kg/s
N	Normal distribution	-
p	Particle	-
Q	Carrier-gas flow rate	m^3/s
R	Weight-fraction of particles	-
R	Universal gas constant	8.3145 J/(K·mol)
R^2	Squared Pearson correlation coefficient	-
t	Time	s
t_{res}	Residence time	s
u_t	Terminal velocity	m/s
V	Volume	m^3
x_i	Input variable *i*	-
y_i	Volume fraction	-
y	Output variable	-
$\hat{y}$	Predicted output variable	-
w	Mass fraction	-
X	Data-matrix	-
β	Mass transfer coefficient	m/s
ρ	Density	kg/m^3

Ω	Fraction of contacted particles	-
θ	Contact angle	^{o}
[ ]	Species dissolved in hot metal	-
( )	Species in slag phase	-
{ }	Species in gas phase	-
< >	Solid species	-
MAE	Mean absolute error of prediction	-
SOS	Sum of squared errors	-

1022

REFERENCES

1. F. Oeters, P. Strohmenger and W. Pluschkell: *Arch. Eisenhüttenwes.* 1979, 44, pp. 727–733.
2. A. F. Shevchenko, A. G. Kiyashko and A. N. Mal´kov:*Steel USSR*, 1984, 14, pp. 116–117.
3. J. Coudure and G. Irons: *ISIJ Int.*, 1994, 34, pp. 155–163.
4. D. Lindström and D. Sichen: *Steel Res. Int.*, 2014, 86, pp. 73–83.
5. G. Irons: *Ironmak. Steelmak.*, 1989,16, pp. 28–36.
6. F. Oeters: Metallurgy of steelmaking, Verlag Stahlheisen, Düsseldorf, Germany, 1994.
7. G. Irons: *ISS Transactions*, 1984, 5, pp. 33–45.
8. F. Harrell: Regression Modeling Strategies: With Applications to Linear Models, Logistic Regression and Survival Analysis, Springer, New York, NY, USA, 2001.
9. W. Ma, H. Li, Y. Cui, B. Chen, G. Liue and J. Ji: *ISIJ Int.* 2017, 57, pp. 214–219.
10. N. Altman and M. Krzywinski: *Nat. Methods*, 2017, 14, pp. 213–214.
11. U. Pal and B. Patil: *Ironmak. Steelmak.* 1986, 13, pp. 294–300.
12. M. Nakano and K. Ito: *ISIJ Int.* 2016, 56, pp. 1537–1542.
13. Y. Zhao and G. Irons: *Ironmak. Steelmak.* 1994, 21, pp. 303–308.
14. D. Lindström, P. Nortier and D. Sichen: *Steel Res. Int.* 2014, 86, pp. 76–88.
15. A. Datta, M. Hareesh, P. Kalra, B. Deo and R. Boom: *Steel Res.*, 1994, 11, pp. 466-471.
16. R. Clift, J. Grace and M. Weber: Bubbles, Drops and Particles, Academic Press, New York, USA, 1978.
17. J. Lee and K. Morita: *ISIJ Int.* 2004, 44, J. Lee and K. Morita, ISIJ Int, 2004, 44, pp. 235–242.
18. D. Lindström and D. Sichen: *Metall. Trans. B*, 2014, 46, pp. 83-92.
19. S. Yousuf, M. Mohamed and S. Maitra:*J. Eng. Sci. Techn.*, 2012, 7, pp. 1–10.
20. G. Sigworth and J. Elliott:*Met. Sci.*, 1974, 8, pp. 298–310.
21. L. Chiang, G. Irons, W. Lu andand I. Cameron: *Iron Steelmaker*, 1990, 17, pp. 35–52.
22. D. Vinoo, D. Mazumdar andS. Gupta: *Ironmak. Steelmak.*, 2007, 34, pp. 471–476.
23. T. Engh, K. Larsen and K. Venås: *Ironmak. Steelmak.*,1979, 6, pp. 268–273.
24. M. Miyata and Y. Higuchi: *ISIJ Int.*, 2017, 57, pp. 1742–1750.

25. Y. Zhao: Doctoral thesis, McMaster University, Hamilton, Ontario, Canada 1992.
26. Y. Jin, X. Bi & S. Yu:*Acta Metall. Sin. (Engl. Lett.)*, 2006, 16, pp. 258–264.
27. S. Weisberg: Applied Linear Regression, John Wiley & Sons, New York, NY, USA 1985.
28. R. Rastogi, K. Deb, B. Deo and R. Boom:*Steel Res.*, 1994, 65, pp. 472–478.
29. B. Deo, A. Datta, B. Kukreja, R. Rastogi and K. Deb:*Steel Res.*, 1994, 65, pp. 528–533.
30. N. Weiss: Elementary Statistics, Addison-Wesley Longman Publishing Co., Inc., Boston, MA, USA, 2007.
31. A. Sen and M. Srivastava, Regression Analysis: Theory, Methods, and Applications, Springer-Verlag, New York, NY, USA, 1990.
32. V. Rashtchi, E. Rahimpour and E. Rezapour: *Electr. Eng.*, 2006, 88, pp. 417–422.
33. H. Tang, X. Xing, W. Dai and Y. Xiao: *J. Hydrodyn.*, 2010, 22, pp. 246–253.
34. M. Jahromi and M. Ameli: *Electr. Pow. Syst. Res.*, 2018, 158, pp. 82–91.
35. L. Lai and J. Ma: *IEEE Trans. Energy Convers.*, 1996, 11, pp. 523–529.
36. L. Yao and W. Sethares: *IEEE Trans. Signal Process.*, 1994, 42, pp. 927–935.
37. R. Picard and D. Cook: *J. Am. Stat. Assoc.*, 1984, 79, pp. 575–583.
38. A. Kumar and G. Roy: *Metall. Mater. Trans. B*, 2005, 36, pp. 901–904.
39. K. McInnon: *SIAM J. Optim.*, 1998, 9, pp. 148–158.
40. M. Dub and R. Jalovecký: Proceedings of the 14th International Power Electronics and Motion Control Conference, 2010, pp. 9–11.
41. T. Sattarpour, D. Nazarpour, S. Golshannavaz and P. Siano: *J. Ambient Intell. Human. Comput.*, 2018, 9, pp. 105–122.
42. A. Gharahbagh and V. Abolghasemi: *WASJ*, 2008, 5, pp. 137–142.
43. H. Dong, H. Wang and S. Chu: *J. S. Afr. Inst. Min. Metall.*, 2014, 114, pp. 489–495.
44. J. Lagarias, J. Reeds, M. Wright and P. Wright: *SIAM J. Optim.*, 1998, 9, pp. 112–147.
45. J. Nelder and R. Mead: *Comput. J.*, 1965, 7, pp. 308–313.
46. MathWorks: fminsearch, https://se.mathworks.com/help/matlab/ref/fminsearch.html. Accessed February 5, 2018.
47. B. Deo and V. Srivastava: *Manuf. Processes*, 2003, 18, pp. 401-408.
48. T. Bäck and M. Schütz, Proceedings of the 9th International Symposium on Methodologies for Intelligent Systems, 1996, pp. 158–167.

49. D. Goldberg: Genetic Algorithms in Search, Optimization, and Machine Learning, Addison-Wesley, Boston, MA, USA, 1989.
50. O. Roeva, S. Fidanova and M. Paprzycki: Proceedings of the 2013 Federated Conference on Computer Science and Information Systems, pp. 371–376.
51. T. Chen, K. Tang, G. Chen and X. Yao: *Theoretical Computer Science*, 2012, 436, pp. 54-70.
52. H.-M. Delhey, E. Schürmann, W. Fix and L. Fiege: Stahl Eisen, 1989, 109, pp. 1207–1214.

Appendix 1: Tables

Table I. Particle size distributions of applied reagents.

Reagent	Particle diameters [µm]									$CaCO_3$ (wt %)	$[S]_0$ [wt %]	$[S]_t$ [wt%]	k (1/min)
	d_{ka}	d_{32}	$d_{A,mean}$	$d_{V,mean}$	d_{90}	d_{80}	d_{50}	d_{25}	d_{10}				
A	55.5	6.7	6.2	67.5	240.0	135.0	26.5	6.2	2.8	9	0.066	0.008	0.22
B	68.6	7.2	6.8	120.4	428.5	223.6	33.8	6.4	3.0	5	0.038	0.014	0.15
C	75.2	7.4	7.4	124.4	410.1	233.6	43.7	7.2	3.2	0	0.047	0.015	0.12
D	18.4	4.3	3.9	37.4	97.9	73.3	24.2	4.1	1.2	0	0.057	0.011	0.18
E	42.1	5.6	5.4	33.8	117.1	69.9	10.4	4.4	2.2	10	0.047	0.007	0.24

Table II. Data-set applied to fitting of the models.

Reagent	T (K)	m_{Fe} (t)	t (min)	Reagent (kg)	$[S]_0$	$[S]_t$
A	1623	60.1	5.6	450.4	0.017	0.005
A	1616	81.4	12.3	703.2	0.104	0.005
A	1634	81.4	10.7	773.1	0.103	0.008
A	1654	78.6	5.6	848.7	0.022	0.011
A	1659	75.7	6.6	578.5	0.034	0.007
A	1606	80.1	8.7	818.0	0.033	0.006
A	1676	72.4	7.8	720.2	0.043	0.008
A	1611	81.7	9.3	634.5	0.078	0.012
B	1693	86.0	5.3	712.8	0.017	0.007
B	1668	84.0	7.7	987.5	0.039	0.014
B	1629	82.3	4.5	740.5	0.030	0.016
B	1673	89.1	5.8	651.5	0.029	0.012
B	1649	83.7	6.6	698.9	0.046	0.020
B	1669	80.0	6.5	624.5	0.034	0.013
B	1618	81.8	4.8	612.0	0.030	0.013
B	1640	91.5	9.6	1030.0	0.063	0.017
C	1649	93.7	7.2	930.0	0.021	0.010
C	1667	79.7	9.4	635.2	0.027	0.009
C	1622	87.3	5.9	908.0	0.027	0.019
C	1635	80.7	12.1	563.3	0.061	0.015
C	1636	87.9	9.4	1357.0	0.060	0.021
C	1623	83.9	9.4	1239.9	0.053	0.018
C	1624	87.1	10.7	638.8	0.061	0.019
D	1649	89.0	9.7	1012.9	0.062	0.010
D	1634	77.7	9.1	1121.0	0.057	0.008
D	1637	88.7	9.8	983.0	0.066	0.013
D	1664	87.5	7.7	564.6	0.046	0.014
D	1674	86.0	9.9	787.0	0.050	0.007
D	1624	77.4	9.5	990.3	0.055	0.009
D	1650	79.0	6.6	1001.3	0.036	0.013
D	1632	81.2	8.2	560.3	0.053	0.013
E	1669	81.3	11.1	727.7	0.047	0.001
E	1649	88.8	10.1	698.5	0.049	0.013
E	1686	80.1	14.0	514.6	0.077	0.005
E	1650	74.4	8.2	867.8	0.041	0.005
E	1660	77.7	6.9	929.0	0.038	0.006
E	1695	82.9	7.2	836.0	0.037	0.007
E	1654	87.9	10.8	711.4	0.048	0.007
E	1711	90.1	9.6	867.0	0.037	0.009
E	1637	81.4	9.1	457.5	0.039	0.007

1136
1137 **Table III. Identified modeling coefficients.**

Method	Cost function	b_0	b_1	b_2	b_3	b_4	R^2	MAE	SOS
MLR – Best solution	Linear	-1.40	0.52	0.70	0.97	0.63	0.90	0.0012	$6.01 \cdot 10^{-5}$
GA – Best solution	Non-linear	-1.34	0.51	0.52	0.81	1.23	0.91	0.0010	$5.81 \cdot 10^{-5}$
Nelder-Mead – Best solution	Non-linear	-2.00	0.39	0.48	0.62	1.07	0.91	0.0011	$5.60 \cdot 10^{-5}$

1138

1139

Table IV. Comparison of prediction approaches for end sulfur content for all the data.

Model	R^2	MAE	d_{res}
Surface area approach (RRS)	0.29	0.0039	35
Surface area approach (Sauter)	0.29	0.0057	1.5
Surface area approach (RRS, Limited contact, Q_{tot})	0.76	0.0020	23
Parameterized rate constant (d_{80})	0.88-0.91	0.0010-0.0012	-

Table V. Results of the external validation.

Method	Cost function	R^2	SOS	MAE [wt-%]
MLR – Best solution	Linear	0.89	$4.2 \cdot 10^{-5}$	0.0012
GA – Best solution	Non-linear	0.91	$3.7 \cdot 10^{-5}$	0.0011
Nelder-Mead – Best solution	Non-linear	0.83	$5.9 \cdot 10^{-5}$	0.0016

Table VI. Summary of the test statistics for 500 repetitions.

Method	Measure	Mean	Median	Best	Worst	Mode
GA – Fit	R^2	0.92	0.92	0.93	0.82	0.92
GA – Fit	MAE	0.0012	0.0012	0.0009	0.0016	0.0012
GA – Validation	R^2	0.85	0.86	0.91	0.68	0.88
GA – Validation	MAE	0.0014	0.0014	0.0010	0.0022	0.0013
Nelder-Mead – Fit	R^2	0.38	0	0.93	0	0
Nelder-Mead – Fit	MAE	0.0072	0.0116	0.0010	0.0116	0.0116
Nelder-Mead – Validation	R^2	0.39	0.29	0.90	0.00	0.83
Nelder-Mead – Validation	MAE	0.0062	0.0095	0.0011	0.0095	0.0095

LIST OF FIGURES